J|A|C|S ARTICLES

Published on Web 10/22/2010

# C−H vs C−C Bond Activation of Acetonitrile and Benzonitrile via Oxidative Addition: Rhodium vs Nickel and Cp* vs Tp′ (Tp′ = Hydrotris(3,5-dimethylpyrazol-1-yl)borate, Cp* = $\eta^5$-Pentamethylcyclopentadienyl)

Meagan E. Evans, Ting Li, and William D. Jones*

*Department of Chemistry, University of Rochester, Rochester, New York 14627, United States*

Received September 2, 2010; E-mail: jones@chem.rochester.edu

***Abstract:*** The photochemical reaction of $(C_5Me_5)Rh(PMe_3)H_2$ (**1**) in neat acetonitrile leads to formation of the C−H activation product, $(C_5Me_5)Rh(PMe_3)(CH_2CN)H$ (**2**). Thermolysis of this product in acetonitrile or benzene leads to thermal rearrangement to the C−C activation product, $(C_5Me_5)Rh(PMe_3)(CH_3)(CN)$ (**4**). Similar results were observed for the reaction of **1** with benzonitrile. The photolysis of **1** in neat benzonitrile results in C−H activation at the ortho, meta, and para positions. Thermolysis of the mixture in neat benzonitrile results in clean conversion to the C−C activation product, $(C_5Me_5)Rh(PMe_3)(C_6H_5)(CN)$ (**5**). DFT calculations on the acetonitrile system show the barrier to C−H activation to be 4.3 kcal mol$^{-1}$ lower than the barrier to C−C activation. A high-energy intermediate was also located and found to connect the transition states leading to C−H and C−C activation. This intermediate has an agostic hydrogen interaction with the rhodium center. Reactions of acetonitrile and benzonitrile with the fragment [Tp′Rh(CNneopentyl)] show only C−H and no C−C activation. These reactions with rhodium are compared and contrasted to related reactions with $[Ni(dippe)H]_2$, which show only C−CN bond cleavage.

## Introduction

The selective cleavage of carbon−hydrogen and carbon−carbon bonds by homogeneous transition metals remains a significant challenge for organometallic chemistry, with cleavage of the latter type of bond proving to be much more difficult. Due to their ready accessibility, kinetic and thermodynamic factors favor carbon−hydrogen bond activation over carbon−carbon bond activation. C−C bonds are sterically less available for activation, and the majority of successful C−C cleavage reactions use relief of strain, proximity, or achievement of aromaticity as the driving force for the reaction.[1]

The past decade, however, has seen some advancement in the area of C−C bond activation in the form of C−CN cleavage (Scheme 1). Our group has been able to activate the C−CN bonds of alkyl and aryl nitriles via oxidative addition to Ni(0) using $[(dippe)NiH]_2$.[2] In this reaction, an $\eta^2$-C,N nitrile complex is formed before the C−CN cleavage product. Also, there is no evidence for oxidative addition of a C−H bond prior to or after the formation of either species, and independent synthesis of $Ni(dippe)(CH_2CN)H$ shows that it is only stable at low temperature (<−40 °C).[2a] Bergman and Brookhart used a cationic rhodium(III) silyl complex[3] that cleaves the C−CN bond of both alkyl and aryl nitriles through an electrophilic addition pathway. Parkin reported C−CN activation by the photolysis of $[Me_2Si(C_5Me_4)_2]MoH_2$ in acetonitrile.[4] Nakazawa has also used iron to break aryl-nitrile C−CN bonds using silanes to remove the cyanide.[5] None of these other complexes shows evidence for C−H bond activation of the nitrile either, although a recent report by Chetcuti showed activation of the C−H bond of acetonitrile on nickel(II) using potassium *tert*-butoxide.[6]

In contrast, the fragment [Tp′Rh(CNneopentyl)] reacts cleanly with acetonitrile to give exclusively the C−H activation product Tp′Rh(CNneopentyl)$(CH_2CN)H$ (eq 1).[7] This compound is thermally robust, and eliminates acetonitrile when heated to 100 °C ($\tau_{1/2}$ = 3 d), with no evidence for C−CN bond activation. These two reactive metal systems feature reactive fragments ([Ni(dippe)] and [Tp′Rh(CNR)]) that are both (1) coordinatively

(1) For reviews of C−C bond activation by organometallic complexes, see:(a) Murakami, M.; Ito, Y. In *Topics in Organometallic Chemistry*; Murai, S. v., Ed.; Springer-Verlag: New York, 1999; pp 97−129. (b) Rybtchinski, B.; Milstein, M. *Angew. Chem., Int. Ed.* **1999**, *38*, 870. (c) Perthuisot, C.; Edelbach, B. L.; Zubris, D. L.; Simhai, N.; Iverson, C. N.; Muller, C.; Satoh, T.; Jones, W. D. *J. Mol. Catal. A* **2002**, *189*, 157. (d) Jun, C. H. *Chem. Soc. Rev.* **2004**, *33*, 610.

(2) (a) Atesin, T. A.; Li, T.; Lachaize, S.; Brennessel, W. W.; Garcia, J. J.; Jones, W. D. *J. Am. Chem. Soc.* **2007**, *129*, 7562. (b) Li, T.; Garcia, J. J.; Brennessel, W. W.; Jones, W. D. *Organometallics* **2010**, *29*, 2430. (c) Garcia, J. J.; Arevalo, A.; Brunkan, N. M.; Jones, W. D. *Organometallics* **2004**, *23*, 3997. (d) Garcia, J. J.; Jones, W. D. *Organometallics* **2000**, *19*, 5544. (e) Garcia, J. J.; Brunkan, N. M.; Jones, W. D. *J. Am. Chem. Soc.* **2002**, *124*, 9547. (f) Atesin, T. A.; Li, T.; Lachaize, S.; Garcia, J. J.; Jones, W. D. *Organometallics* **2008**, *27*, 3811.

(3) (a) Taw, F. L.; White, P. S.; Bergman, R. G.; Brookhart, M. *J. Am. Chem. Soc.* **2002**, *124*, 4192. (b) Taw, F. L.; Mueller, A. H.; Bergman, R. G.; Brookhart, M. *J. Am. Chem. Soc.* **2003**, *125*, 9808.

(4) Churchill, D.; Shin, J. H.; Hascall, T.; Hahn, J. M.; Bridgewater, B. M.; Parkin, G. *Organometallics* **1999**, *18*, 2403.

(5) Nakazawa, H.; Kamata, K.; Itazaki, M. *Chem. Commun.* **2005**, 4004. Nakazawa, H.; Kawasaki, T.; Miyoshi, K.; Suresh, C. H.; Koga, N. *Organometallics* **2004**, *23*, 117.

(6) Oertel, A. M.; Ritleng, V.; Chetcuti, M. J.; Veiros, L. F. *J. Am. Chem. Soc.* **2010**, *132*, 13588.

(7) Vetter, A. J.; Rieth, R. D.; Jones, W. D. *Proc. Natl. Acad. Sci. U.S.A.* **2007**, *104*, 6957.



**10.1021/ja107927b** 

***Scheme 1.*** Recent Examples of C−CN Cleavage

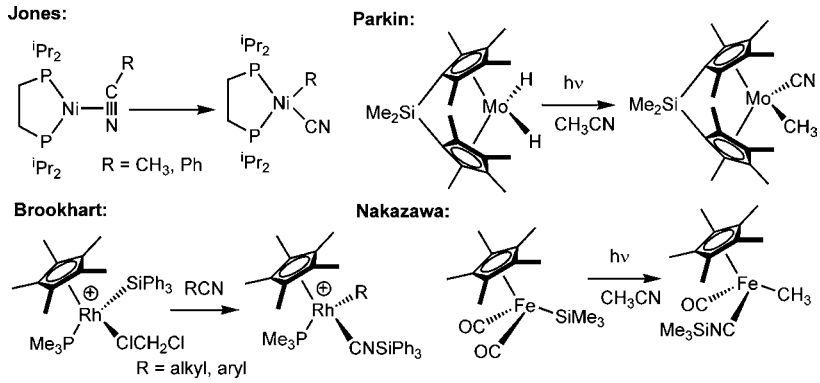


unsaturated, (2) low-valent, and (3) prone to oxidative addition to give stable $d^8$-square planar and $d^6$-octahedral products, respectively. Why, then, does nickel cleave exclusively the C−CN bond, whereas rhodium cleaves exclusively the C−H bond? If the same driving forces exist, why is the selectivity displayed by these metals so distinct?

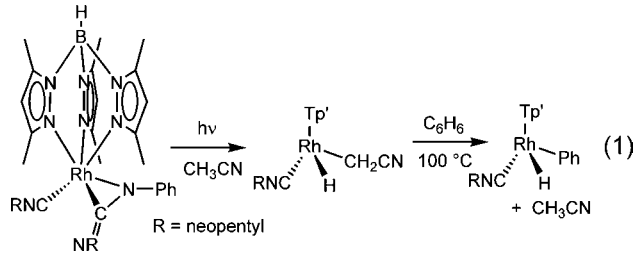


To address this issue, we chose to use $(C_5Me_5)Rh(PMe_3)H_2$ in the current study to examine the possibility of C−H and/or C−C activation of acetonitrile and benzonitrile, taking advantage of the well-documented relationship between Cp* and Tp′ complexes, and to elucidate further the differences between the [Ni(dippe)] and [Tp′Rh(CNR)] fragments. This Cp* complex has already shown remarkable selectivity for the activation of C−H bonds of aliphatic and aromatic hydrocarbons,[8] and for cleavage of C−S[9] and C−F bonds.[10]

## Results and Discussion

**Reactivity of [$(C_5Me_5)Rh(PMe_3)$] toward Acetonitrile and Benzonitrile.** Irradiation of $(C_5Me_5)Rh(PMe_3)H_2$ (**1**) results in the loss of dihydrogen, producing the 16-electron coordinatively and electronically unsaturated metal fragment, $[(C_5Me_5)Rh(PMe_3)]$. When this irradiation was carried out in acetonitrile, the unsaturated rhodium center inserted into the C−H bonds of acetonitrile producing $(C_5Me_5)Rh(PMe_3)(CH_2CN)H$ (**2**) in near quantitative yield (NMR) at 75% conversion (Scheme 2), similar to what was seen with the Tp′RhL fragment. Longer photolysis times did not lead to higher conversion of **1** to **2**, but instead led to formation of the Rh(I) species, $(C_5Me_5)Rh(PMe_3)_2$, and presumably unobserved "Cp*Rh" decomposition products. The most notable resonance in the $^1$H NMR spectrum of **2** is that for the hydride which appears as a doublet of doublets at $\delta$ −13.766 ($J_{Rh-H}$ = 41.7 Hz, $J_{P-H}$ = 27.4 Hz). The $C_5Me_5$ and $PMe_3$ proton resonances appear at $\delta$ 1.70 and 1.04, respectively.

***Scheme 2.*** Reactions of **1** with Acetonitrile

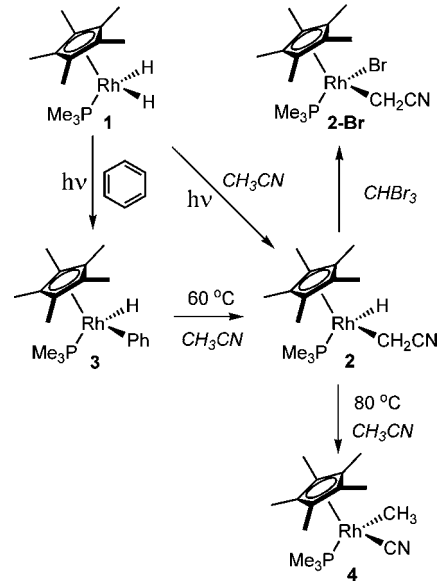


The $CH_2CN$ protons were not observed in the $^1$H NMR spectrum most likely due to the multiple couplings between the diastereotopic protons, rhodium and phosphorus. The $^{31}P\{^1H\}$ NMR spectrum for **2** appears as a doublet at $\delta$ 6.67 ($J_{Rh-P}$ = 149 Hz), similar to other rhodium(III) monophosphine compounds.[7,11,12]

Further characterization of **2** was made possible by quenching it with $CHBr_3$ and converting it into the air-stable bromide derivative, $(C_5Me_5)Rh(PMe_3)(CH_2CN)Br$ (**2-Br**). The $^{31}P\{^1H\}$ NMR spectrum of **2-Br** displays a doublet at $\delta$ 3.47 ($J_{Rh-P}$ = 146 Hz) slightly upfield of the dibromide complex ($\delta$ 3.73, $J_{Rh-P}$ = 137 Hz), which was formed from residual **1**. The $^1$H NMR spectra for **2-Br** displays resonances at $\delta$ 1.75 and 1.58 for the $C_5Me_5$ and $PMe_3$ protons. Its structure was also confirmed by single crystal X-ray diffraction, shown in Figure 1a. The $^1$H−$^{13}$C HSQC experiment allowed the identification of the C$H_2$CN protons as a broad resonance at $\delta$ 1.53 in the $^1$H NMR spectrum, correlated to a doublet of doublets at $\delta$ −14.20 ($J$ = 13.8 and 26.6 Hz) in the $^{13}$C NMR spectrum.

Low-temperature photolysis studies were also performed in an attempt to observe any possible $\eta^1$- or $\eta^2$-nitrile intermediates (as seen with [Ni(dippe)]). Compound **1** was irradiated in neat acetonitrile at −40 °C for 5 min and immediately monitored by $^{31}P\{^1H\}$ NMR spectroscopy in a precooled NMR probe set to −40 °C. At this temperature, no rhodium(I) species were

(8) Jones, W. D.; Feher, F. J. *J. Am. Chem. Soc.* **1984**, *106*, 1650. Jones, W. D.; Feher, F. J. *Acc. Chem. Res.* **1989**, *22*, 91.
(9) (a) Atesin, T. A.; Jones, W. D. *Organometallics* **2008**, *27*, 3666. (b) Atesin, T. A.; Jones, W. D. *Inorg. Chem.* **2008**, *47*, 10889.
(10) Edelbach, B. L.; Jones, W. D. *J. Am. Chem. Soc.* **1997**, *119*, 7734.
(11) Jones, W. D.; Feher, F. J. *J. Am. Chem. Soc.* **1984**, *23*, 2376.
(12) Jones, W. D.; Kuykendall, V. L. *Inorg. Chem.* **1991**, *30*, 2615.

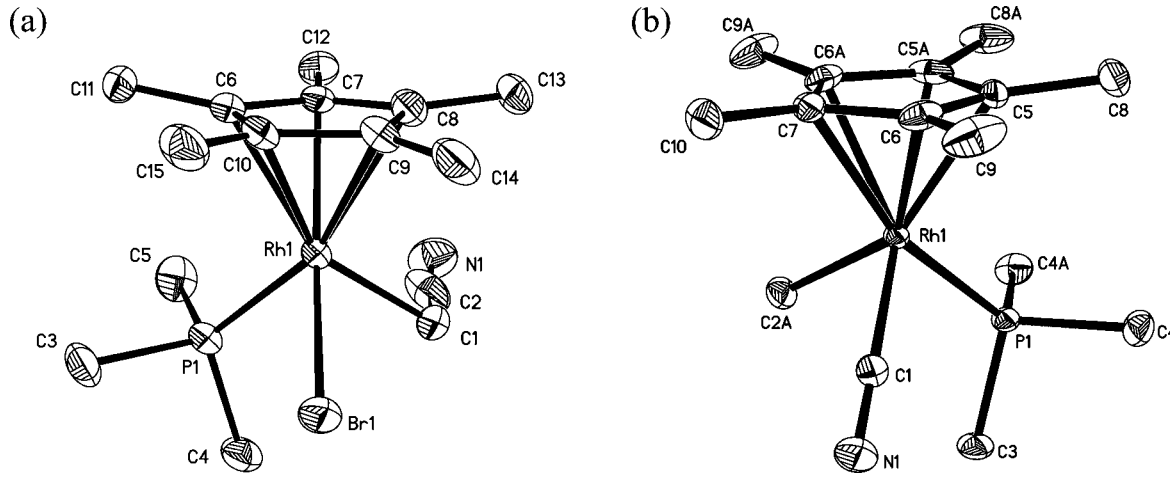


***Figure 1.*** (a) Thermal ellipsoid drawing of Cp*Rh($PMe_3$)($CH_2CN$)Br (**2-Br**). Ellipsoids are shown at the 50% probability level. Hydrogen atoms have been omitted for clarity. Selected bond lengths (Å): Rh(1)−Br(1), 2.5398; Rh(1)−C(1), 2.108; C(1)−C(2), 1.430; C(2)−N(1), 1.150; Rh(1)−P(1), 2.2813. Selected angles (deg): Br(1)−Rh(1)−C(1), 87.08; C(1)−C(2)−N(1), 178.9. (b) Thermal ellipsoid drawing of Cp*Rh($PMe_3$)($CH_3$)(CN) (**4**). Ellipsoids are shown at the 50% probability level. Hydrogen atoms have been omitted for clarity. Selected bond lengths (Å): Rh(1)−C(1), 1.959; Rh(1)−C(2A), 2.124; C(1)−N(1), 1.160; Rh(1)−P(1), 2.2566. Selected angles (deg): C(2A)−Rh(1)−C(1), 84.5; Rh(1)−C(1)−N(1), 178.6.

observed. Only the C−H activation complex **2** and unreacted compound **1** were observed.

The acetonitrile C−H activation complex was also produced under thermal conditions. Complex **3**, ($C_5Me_5$)Rh($PMe_3$)(Ph)H, is known to eliminate benzene at 60 °C with a half-life of ∼1 h.[7] Upon heating **3** to 60 °C for 3 h in neat acetonitrile, the major product was the C−H activation complex **2**. However, a new species was observed as a minor product with proton resonances at $\delta$ 1.51 and 0.98, corresponding to the protons of $C_5Me_5$ and $PMe_3$ ligands, along with a doublet of doublets at $\delta$ 0.49 ($J_{Rh-H}$ = 5.8 Hz, $J_{P-H}$ = 2.3 Hz). This new product was identified as the C−C activation product, ($C_5Me_5$)Rh($PMe_3$)($CH_3$)(CN) (**4**). Continued heating of this solution resulted in complete conversion of the C−H activation product to the C−C activation product, establishing the latter as being thermodynamically preferred. Complex **4** is air-stable and was fully characterized both by NMR spectroscopy and by single-crystal X-ray diffraction (Figure 1b). The $^{31}P\{^1H\}$ NMR spectrum of **4** displays as a doublet at $\delta$ 8.56 ($J_{Rh-P}$ = 141 Hz). The $^{13}C\{^1H\}$ NMR spectrum displays resonances for the $CH_3$ and CN groups as doublets of doublets at $\delta$ −7.78 and 136.9, respectively.

The mechanism for the conversion of the C−H activation product (**2**) to the C−C activation product (**4**) was examined by dissolving a sample of **2** and **4** (7:1 ratio) in acetonitrile-$d_3$ followed by heating at 80 °C. The resonance for the Rh−Me group of compound **4** was monitored over time (relative to an integration standard) and was found to grow in as the hydride resonance of **2** disappeared, even in the presence of acetonitrile-$d_3$. From integration of the hydride and methyl resonances, only about 5% of the C−H activation compound underwent dissociation of acetonitrile from rhodium prior to C−CN cleavage. This was most evident in the $^{31}P\{^1H\}$ NMR spectrum, which displayed deuterium splitting on the C−H activation complex in a minor amount (Figure 2). The majority of compound **2** rearranged to **4** without dissociating acetonitrile from the rhodium center (eq 2).

Similar results were observed for the reactions of benzonitrile with [($C_5Me_5$)Rh($PMe_3$)]. Photolysis of **1** in neat benzonitrile led to C−H activation at the ortho, meta, and para positions

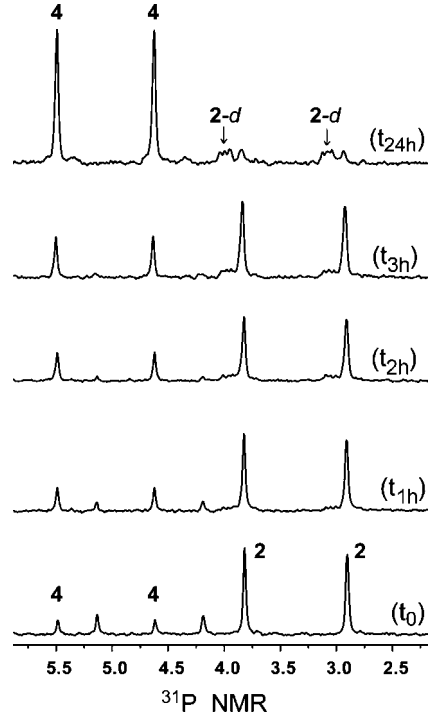


***Figure 2.*** $^{31}P\{^1H\}$ NMR spectra for thermal rearrangement of **2** to **4** in the presence of $CD_3CN$. Notice the small amount of deuterium coupling in compound **2-*d*** due to the formation of a small quantity of Cp*Rh($PMe_3$)($CD_2CN$)D. The majority of **2** rearranges to **4** without dissociating from rhodium.

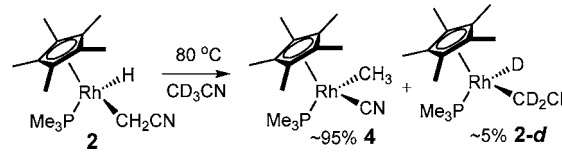


(2)

(eq 3). The $^1H$ NMR spectrum showed the presence of three hydrides as doublets of doublets at $\delta$ −12.86, −13.84, and −13.85. The $^{31}P\{^1H\}$ NMR spectrum showed the presence of five new compounds each as a doublet with $J_{Rh-P}$ between 146 and 149 Hz, indicative of Rh(III) species (assigned para, meta,

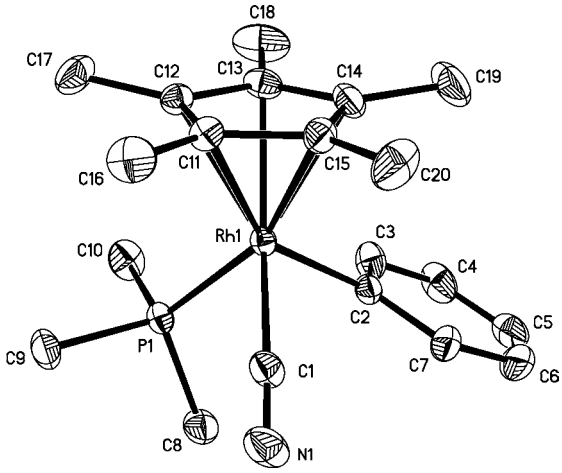


***Figure 3.*** Thermal ellipsoid drawing of $(C_5Me_5)Rh(PMe_3)(Ph)(CN)$ (**5**). Ellipsoids are shown at the 50% probability level. Hydrogen atoms have been omitted for clarity. Selected bond lengths (Å): Rh(1)−C(1), 1.9819; Rh(1)−C(2), 2.0579; C(1)−N(1), 1.165; Rh(1)−P(1), 2.2590. Selected angles (deg): C(2)−Rh(1)−C(1), 91.37; Rh(1)−C(1)−N(1), 176.03.

and ortho isomers plus rotamers of ortho and meta). Heating this mixture of products in neat benzonitrile led to the disappearance of all C−H activation products and complete conversion to the C−C activation product, $(C_5Me_5)Rh(PMe_3)(Ph)(CN)$ (**5**). Product **5** was separated from benzonitrile by prep TLC. The $^1$H NMR spectrum for **5** shows the $C_5Me_5$ and $PMe_3$ resonances at $\delta$ 1.74 and 1.35, respectively. The $^{31}P\{^1H\}$ NMR spectrum shows a doublet at $\delta$ 13.02 (d, $J_{Rh-P} = 135$ Hz). The $^{13}C\{^1H\}$ NMR spectrum shows the $PMe_3$ carbons as a doublet at $\delta$ 16.19, the $C_5Me_5$ carbons at $\delta$ 9.81 and 100.40, and the CN carbon as a doublet of doublets at $\delta$ 153.36. The ipso carbon of the phenyl ring appears as a doublet of doublets at $\delta$ 138.39, with the ortho, meta, and para carbons appearing at $\delta$ 140.70, 128.17, and 122.79. The X-ray structure is shown in Figure 3.

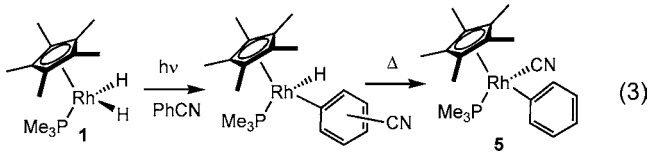

(3)

**Reactivity of [Tp′RhL] toward Acetonitrile and Benzonitrile.** As mentioned above, the photolysis of Tp′Rh(CNR)(carbodiimide) in neat acetonitrile cleanly produces the C−H activation product, Tp′RhL($CH_2CN$)H.[6] The $^1$H NMR spectrum for this compound has a hydride resonance at $\delta$ −14.33 (d, $J_{Rh-H} = 20$ Hz) and two resonances for the diastereotopic methylene hydrogens of the $CH_2CN$ ligand. While the fragment [Tp′Rh(CNR)] shows good reactivity toward the C−H bonds of alkyl nitriles,[7] no cleavage of the C−CN bonds has been observed. In light of the new results showing a strong thermodynamic preference of $[(C_5Me_5)Rh(PMe_3)]$ for the cleavage of C−C bonds, we wanted to test the selectivity of the [Tp′Rh(CNR)] system on acetonitrile under more forcing conditions to see if it could be converted to the anticipated C−CN cleavage product. When a sample of Tp′RhL($CH_2CN$)H was then heated at 80 °C for 1 month in neat acetonitrile, no further reaction was observed (eq 4). Heating the sample in neat acetonitrile at 100 or 130 °C for several days only resulted in decomposition to give unidentified products.

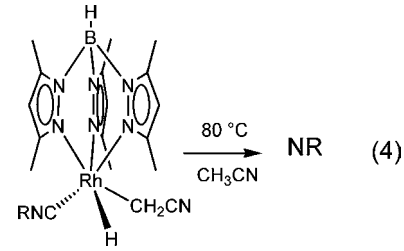

(4)

Likewise, photolysis of Tp′Rh(CNR)(carbodiimide) in neat benzonitrile cleanly produces three C−H activation products, assigned to ortho, meta, and para isomers of Tp′RhL($C_6H_4CN$)H. The $^1$H NMR spectrum for this mixture shows doublets at $\delta$ −13.76, −14.20, and −14.27 with coupling constants of 23.3, 23.3, and 24.7 Hz. Heating this mixture at 160 °C for 3 days led to decomposition. Heating at 100 °C also shows decomposition, but at a slower rate.

These new experiments suggest the importance of the $\sigma$-donating $PMe_3$ as opposed to the $\pi$-accepting isocyanide ligand, although the Tp′ ligand is also changed to Cp* in the current study. Work in progress indicates that it is the phosphine substitution, not the Tp′ substitution, that is critical to the increased reactivity.[13] Furthermore, earlier attempts to prepare the 16 $e^-$ fragment [Cp*Rh(CNR)] indicated that this species could not even activate the C−H bonds of benzene, also pointing to reduced C−C activation capability of the isonitrile derivatives.[14] The requirement of an electron-rich metal center for C−C activation is consistent with previous results obtained with the [Ni(dippe)] system, which has an electron-rich metal center and shows only C−C activation.[15]

**Computational Results.** Due to the fact that the energetics for C−H and C−C bond activation of acetonitrile could not be experimentally determined, density functional theory (DFT) calculations were used to determine the reaction pathways and transition states for both bond activations. Optimized structures are shown in Figure 4. Selected structural parameters for each of the optimized stationary points are shown in Table I, displaying good agreement with the available experimental data. Movies are included in the Supporting Information for both C−H and C−C cleavage. The optimized geometry for the C−C activation product (**S1**) has a Rh−C1 bond length of 1.97 Å and a Rh−C2 bond length of 2.11 Å, similar to the X-ray structural data for **4** which has corresponding bond lengths of 1.96 Å and 2.12 Å. Likewise, **S5** has a Rh−C2 bond length of 2.13 Å and **2-Br** has a Rh−C1 bond length of 2.11 Å.

Initially, the energies for stationary points **S1** and **S5** were calculated. It was found that **S1** lies 8.1 kcal $mol^{-1}$ lower in energy than **S5** as shown in Figure 5. The relative energy of these two species is in agreement with experimental observations, in which the C−C activation product is thermodynamically preferred over the C−H activation product. The energies for both the $\eta^2$-nitrile (**S6**) and $\eta^1$-nitrile (**S7**) species were calculated even though neither was observed in the reaction. The results show that the C−H activation product (**S5**) lies slightly lower in energy than **S6** and **S7** by 0.1 kcal $mol^{-1}$ and

(13) Tanabe, T.; Evans, M. E.; Brennessel, W. W.; Jones, W. D. C−H and C−CN Bond Activation of Acetonitrile and Succinonitrile by [Tp′Rh($PR_3$)]. *Organometallics* **2010**, *29*. Submitted.
(14) Jones, W. D.; Duttweiler, R. P.; Feher, F. J.; Hessell, E. T. *Nouv. J. Chem.* **1989**, *13*, 725. Jones, W. D.; Duttweiler, R. P.; Feher, F. J. *Inorg. Chem.* **1990**, *29*, 1505.
(15) Atesin, T. A.; Li, T.; Lachaize, S.; Brennessel, W. W.; Garcia, J. J.; Jones, W. D. *J. Am. Chem. Soc.* **2007**, *129*, 7562.

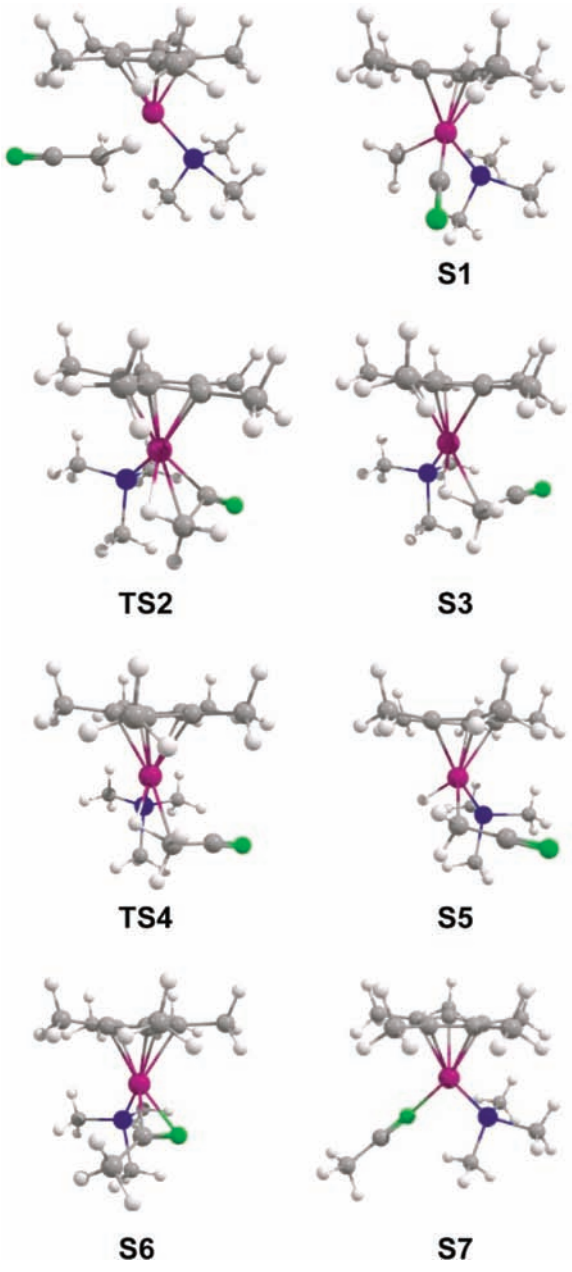


***Figure 4.*** Optimized structures of stationary points on the $[(C_5Me_5)Rh(PMe_3)] + CH_3CN$ potential energy surface. Compounds **S6** and **S7** do not connect to any other species and were not observed in any of the experiments.

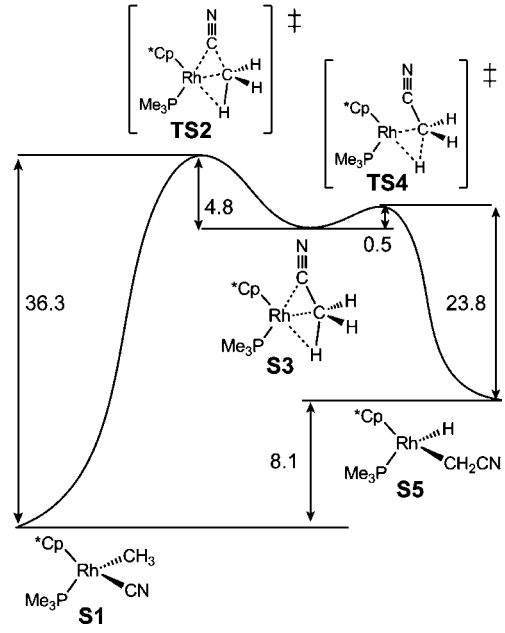


***Figure 5.*** Energetics of C−H and C−C bond activation of acetonitrile by $[(C_5Me_5)Rh(PMe_3)]$ (free energies in kcal mol$^{-1}$ at 298 K, gas phase). All energies are relative to the C−C activation product (**S1**). The energy of the free fragment + acetonitrile is 87.2 kcal mol$^{-1}$.

0.6 kcal mol$^{-1}$, respectively, which suggests that they might be observed experimentally. Due to the fact that acetonitrile was not only a reactant but also the solvent in the reactions, and the fact that acetonitrile is very polar (dipole moment = 14.3 D), the inclusion of a solvent correction dramatically changed the energetics for these species. Using a polarizable continuum model (PCM) correction, the energy for the C−H activation product was lowered dramatically with respect to the $\eta^1$-nitrile and $\eta^2$-nitrile species; making **S5** lower in energy than **S6** and **S7** by 1.9 and 9.1 kcal mol$^{-1}$, respectively.

By doing a potential energy surface scan beginning with the C−C activation product **S1** and pulling one of the methyl hydrogen atoms close to the metal center, transition states and a high-energy intermediate species were found. The intermediate species (**S3**) connects the transition state leading to C−H activation (**TS4**) and the transition state leading to C−C activation (**TS2**). This stable, high-energy species can be described as an $\eta^3$-H,C,C-acetonitrile complex containing an agostic C−H interaction with the metal center. The hydrogen is 1.75 Å from rhodium, and the C−H bond is lengthened to 1.18 Å; the C−C−N angle is bent to 177.15°. Species **S3** lies in a shallow well only 0.5 kcal mol$^{-1}$ below **TS4** and 4.8 kcal mol$^{-1}$ below **TS2**. This very small barrier to C−H activation accounts for the kinetic preference for C−H activation. When the solvent correction was applied to the transition states, the barrier to C−C activation rose to 38.6 kcal mol$^{-1}$, whereas the barrier to C−H bond formation rose to 40.3 kcal mol$^{-1}$, making the barrier to C−C activation lower than the barrier to C−H activation. Note that this situation was *not* in agreement with our experimental observation but is the only place where disagreement was found.

***Table I.*** Optimized Structural Parameters (Å, deg) and Relative Free Energies ($\Delta G$, kcal/mol) of Stationary Points on the $[(C_5Me_5)Rh(PMe_3)] + CH_3CN$[a] Potential Energy Surface (atom numbering is as shown in Figure 1b), Gas Phase (B3LYP)

| | Rh−C1 (Rh−CN) | Rh−C2 (Rh−Me) | C1−C2 | Rh−H[b] | N−C1 | N−C1−C2 | Rh−C1−N | $\Delta G$ |
|---|---|---|---|---|---|---|---|---|
| **S1** | 1.97 | 2.11 | 2.79 | 2.63 | 1.17 | 133.47 | 177.53 | 0.0 |
| **TS2** | 2.00 | 2.36 | 1.68 | 2.22 | 1.19 | 132.45 | 148.39 | 36.3 |
| **S3** | 2.70 | 2.45 | 1.46 | 1.75 | 1.17 | 170.12 | 125.41 | 31.5 |
| **TS4** | 2.82 | 2.37 | 1.45 | 1.67 | 1.17 | 175.48 | 127.13 | 32.0 |
| **S5** | 2.95 | 2.13 | 1.45 | 1.56 | 1.17 | 176.30 | 133.93 | 8.1 |
| **S6** | 2.06 | 3.33 | 1.49 | 3.60 | 1.22 | 141.31 | 78.92 | 8.3 |
| **S7** | 3.14 | 4.59 | 1.48 | 5.07 | 1.17 | 179.38 | 175.44[c] | 8.9 |

[a] Optimized structural parameters (Å, deg) for free acetonitrile: N−C1, 1.16; C1−C2, 1.46; N−C1−C2, 179.85. [b] Shortest Rh−H distance. [c] Angle measure is Rh−N−C1.

When comparing DFT calculations done on both the [($C_5Me_5$)Rh($PMe_3$)] and [Ni(dippe)] systems,[2a] some parallels can be drawn. Most notable is the similarity in the transition state for C−C activation of acetonitrile. In both systems, the C1−C2 bond distance in the transition state for C−C cleavage is 1.68 Å, indicating that the C−C bond is only partially broken in the transition state (cf. C1−C2 in free acetonitrile: 1.46 Å). The differences in free energies between the C−H and C−C activation products in the [($C_5Me_5$)Rh($PMe_3$)] and [Ni(dippe)] systems are 8.1 and 15.3 kcal $mol^{-1}$, respectively. In the rhodium system, the Rh−$CH_3$ bond is 2.36 Å in transition state **TS2** (vs 2.11 Å in product **S1**), and the Rh−CN bond is 2.00 Å in transition state **TS2** (vs 1.97 Å in product **S5**). These parameters indicate a substantial amount of Rh−C bond formation but only a little C−C bond cleavage in the transition state for C−C cleavage. In contrast, the nickel−dmpe system shows a higher degree of bond formation (Ni−$CH_3$: 2.12 Å in TS vs 1.96 Å in the product; Ni−CN: 1.82 Å in TS vs 1.88 Å in the product), but a similar degree of bond breaking (C−CN: 0.22 Å lengthening in TS). DFT analysis of the C−C cleavage of benzonitrile by [Ni(dmpe)] also indicates almost complete Ni−C bond formation with little C−CN bond breaking.[2f]

In addition, DFT calculations on both systems reacting with acetonitrile found a stable, high-energy species that lies between the C−C and C−H transition states. These intermediates in both systems can be described as a weakly bound $\sigma$ C−C bond combined with an agostic C−H interaction. In the nickel system, this intermediate is in a shallow local minimum only 0.9 kcal $mol^{-1}$ lower in energy than the TS leading to the $\eta^2$-nitrile complex. In the rhodium system, the intermediate lies in a shallow local minimum only 0.5 kcal $mol^{-1}$ lower in energy than the TS leading to C−H activation. Calculations on the rhodium system did not identify a pathway from either the $\eta^2$-nitrile or $\eta^1$-nitrile species to either C−H or C−C activation which differs from the nickel example where the $\eta^2$-nitrile complex was identified as a stationary point on the energy landscape.

## Conclusions

The photochemical reaction of **1** in neat acetonitrile led to exclusive formation of the C−H activation product, **2**. Heating a solution of **2** in neat acetonitrile led to rearrangement of the C−H activation product to the C−C activation product **4**. The conversion of **2** to **4** was monitored in acetonitrile-$d_3$, which showed only ∼5% crossover with the majority of the C−H activation product remaining coordinated to the rhodium on the path to C−C activation. The experimental data along with density functional theory calculations show C−H activation is kinetically preferred while C−C activation is thermodynamically preferred. Gas-phase DFT calculations identify **4** (**S1**) to be 8.1 kcal $mol^{-1}$ lower in energy than **2** (**S5**). These calculations also identify a stable high-energy species (a rhodium complex with an agostic hydrogen interaction) in a shallow well between the C−H and C−C transition states. This work represents the first example of C−CN bond activation via oxidative addition to a Rh(I) center and provides new insight into the importance of the $\sigma$-donating ability of the $PMe_3$ ligand. The calculations indicate that the $\eta^2$-C,N acetonitrile complex with rhodium is ∼9 kcal $mol^{-1}$ less favorable than the C−CN cleavage product (PCM corrected), which accounts for its absence in the experiments. With [Ni(dippe)], however, the $\eta^2$-C,N acetonitrile complex is only 2 kcal $mol^{-1}$ less stable than the C−CN cleavage product, and hence it is observed. The instability of the nickel C−H activation product Ni(dippe)($CH_2CN$)H can be attributed to the presence of a weaker Ni−H bond compared to a stronger Rh−H bond in Cp*Rh($PMe_3$)($CH_2CN$)H, rendering C−H activation the kinetically preferred pathway with rhodium. The lack of C−CN cleavage by [Tp′Rh(CNR)] apparently arises because the kinetic barrier to cleavage is sufficiently high that decomposition occurs preferentially at elevated temperatures.

## Experimental Section

**General Procedures.** All operations and routine manipulations were performed under a nitrogen atmosphere, either on a high-vacuum line using modified Schlenk techniques or in a Vacuum Atmospheres Corp. Dri-Lab. Acetonitrile and benzonitrile were purchased from Aldrich Chemical Co. Prior to use they were dried over potassium carbonate and then distilled under vacuum into Teflon-sealed Schlenk flasks where they were stored. Benzene-$d_6$, chloroform-$d_1$, and acetonitrile-$d_3$ were purchased from Cambridge Isotope. Benzene-$d_6$ was distilled under vacuum from a dark-purple solution of benzophenone ketyl and stored in a Teflon-sealed Schlenk flask. Chloroform-$d_1$ was dried over $CaCl_2$ and then vacuum distilled into a Teflon-sealed Schlenk flask. Acetonitrile-$d_3$ was dried over potassium carbonate and distilled under vacuum into a Teflon-sealed Schlenk flask where it was stored. Bromoform was purchased from Aldrich Chemical Co. Prior to use it was dried over calcium chloride and vacuum distilled into a Teflon-sealed Schlenk flask where it was stored. Preparation of Cp*Rh($PMe_3$)$H_2$ (**1**) and Cp*Rh($PMe_3$)($C_6H_5$)H (**3**) have been previously reported.[16,8]

All photolysis experiments were performed using an Oriel 200 W Hg(Xe) arc lamp fitted with a water-filled IR filter. Low temperatures were maintained with a methanol/$N_2$ solution in a Pyrex dewar. All $^1$H, $^{13}$C{$^1$H}, and $^{31}$P{$^1$H} NMR were collected on a Bruker 400 MHz spectrometer in benzene-$d_6$ unless otherwise stated. All chemical shifts were reported in ppm ($\delta$) relative to tetramethylsilane and referenced to the chemical shifts of residual solvent resonances ($C_6H_6$, $\delta$ 7.16; $CHCl_3$, $\delta$ 7.26; $CH_3CN$, $\delta$ 1.94).[17] $^{31}$P{$^1$H} NMR spectra are relative to external reference 85% $H_3PO_4$. Elemental analysis was performed by Dr. William W. Brennessel at the University of Rochester using a Perkin-Elmer 2400 series II elemental analyzer in CHN mode. Mass spectrometry was performed on a Shimadzu LCMS-2010 analyzer.

**Computational Details.** The X-ray crystallographic structures for **2-Br** and **4** were used as the starting points for the calculations. The gas-phase structures were fully optimized in redundant internal coordinates,[18] with density functional theory (DFT) and a wave function incorporating Becke's three-parameter hybrid functional (B3),[19] along with the Lee−Yang−Parr correlation functional (LYP).[20] All calculations were performed using the Gaussian03 package.[21] The Rh and P atoms were represented with the effective core pseudopotentials of the Stuttgart group and the associated basis sets improved with a set of f-polarization functions for Rh ($\alpha$ = 1.350)[22] and a set of d-polarization functions for P ($\alpha$ = 0.387).[23] The remaining atoms (C, H, and N) were represented by a 6-31G(d,p)[24] basis set. The geometry optimizations were performed without any symmetry constraints, and the local minima and the

(16) Isobe, K.; Bailey, P. M.; Maitlis, P. M. *J. Chem. Soc., Dalton Trans.* **1981**, 2003.
(17) Gottlieb, H. E.; Kotlyar, V.; Nudelman, A. *J. Org. Chem.* **1997**, *62*, 7512.
(18) Peng, C.; Ayala, P. Y.; Schlegel, H. B.; Frisch, M. J. *J. Comput. Chem.* **1996**, *17*, 49.
(19) Becke, A. D. *J. Chem. Phys.* **1993**, *98*, 5648.
(20) Lee, C.; Yang, W.; Parr, R. G. *Phys. Rev. B* **1988**, *37*, 785.
(21) Frisch, M. J.; et al. *Gaussian03*; Gaussian, Inc.: Wallingford, CT, 2004.
(22) Ehlers, A. W.; Bohme, M.; Dapprich, S.; Gobbi, A.; Hollwarth, A.; Jonas, V.; Köhler, K. F.; Stegmann, R.; Veldkamp, A.; Frenking, G. *Chem. Phys. Lett.* **1993**, *208*, 111.
(23) Hollwarth, A.; Bohme, M.; Dapprich, S.; Ehlers, A. W.; Gobbi, A.; Jonas, V.; Köhler, K. F.; Stegmann, R.; Veldkamp, A.; Frenking, G. *Chem. Phys. Lett.* **1993**, *208*, 237.
(24) Hehre, W. J.; Ditchfield, R.; Pople, J. A. *J. Chem. Phys.* **1972**, *56*, 2257.

transition-states were checked by frequency calculations. For each transition-state structure, the intrinsic reaction coordinate (IRC) routes were calculated in both directions toward the corresponding minima. For one of the transition states, the IRC calculations failed to reach the energy minima on the potential energy surface; therefore, in those cases geometry optimizations were carried out as a continuation of the IRC path. Because of the polarity of the structures, the solvent effects on their relative stabilities were evaluated by calculating the free energies of the solvation in terms of the polarizable continuum model (PCM). The self-consistent reaction field (SCRF) calculations using the PCM-UA0 solvation model[25] were carried out for the gas-phase optimized structures as well as the PCM optimized structures. The dielectric constant in the PCM calculations was set to $\varepsilon = 36.64$ to simulate acetonitrile as the solvent medium used in the experimental study. Gibbs free energies have been calculated at 298.15 K and 1 atm.

**Preparation of $(C_5Me_5)Rh(PMe_3)(CH_2CN)H$ (2) by Two Methods. Method 1**: A solution of **1** (30 mg, 0.095 mmol) was dissolved in 3 mL of benzene added to a Schlenk flask sealed with a Teflon cap. This solution was then irradiated for 1.5 h at room temperature. The solvent was immediately removed *in vacuo*, yielding compound **3** as a red/brown residue. This product was dissolved in $CH_3CN$ and heated to 60 °C for 3 h. Volatiles were again removed *in vacuo*, yielding **2** and **4** which were dissolved in $C_6D_6$. **Method 2**: A solution of **1** (15 mg, 0.047 mmol) was dissolved in 0.4 mL of acetonitrile and irradiated for 30 min at room temperature. The solvent was immediately removed *in vacuo*, yielding **2** (75% by NMR) as a red/brown residue, which was dissolved in $C_6D_6$ and characterized by NMR spectroscopy. $^1$H NMR ($C_6D_6$): $\delta$ −13.766 (dd, $J_{Rh-H} = 41.7$ Hz, $J_{P-H} = 27.4$ Hz), 1.044 (d, $J_{P-H} = 10.1$ Hz) and 1.702 (d, $J_{Rh-H} = 2.5$ Hz). $^{31}P\{^1H\}$ ($C_6D_6$): $\delta$ 6.665 (d, $J_{Rh-P} = 149$ Hz).

**Preparation of $(C_5Me_5)Rh(PMe_3)(CH_2CN)Br$ (2-Br).** A solution of **1** (100 mg, 0.972 mmol) was dissolved in 3 mL of acetonitrile and irradiated for 60 min at room temperature. The solvent was removed *in vacuo*, leaving a mixture of **2** and unreacted **1** which was then dissolved in benzene. This solution was then quenched with 0.65 mL of a 25% v/v $CHBr_3$/THF solution (1.87 mmol $CHBr_3$). The mixture instantly changed from brown to orange-red upon addition of bromoform solution. Volatiles were again removed, leaving an orange-red solid which was separated by prep TLC using a 1:1 THF/hexane solution. Two bands were observed and collected which were identified as $Cp^*Rh(PMe_3)Br_2$ (yield: 48% by NMR) and $Cp^*Rh(PMe_3)(CH_2CN)Br$ (**2-Br**, yield: 52% by NMR). NMR characterization of $Cp^*Rh(PMe_3)Br_2$ matched previously reported data. For **2-Br**, $^1$H NMR ($C_6D_6$): $\delta$ 1.53 (br, 2 H, $CH_2CN$), 1.576 (d, $J_{P-H} = 10.5$ Hz, 9 H, $PMe_3$) and 1.746 (d, $J_{Rh-H} = 2.9$ Hz, 15 H, $C_5Me_5$). $^{13}C\{^1H\}$ ($CDCl_3$): $\delta$ −14.200 (dd, $J_{Rh-C} = 13.8$ Hz, $J_{P-C} = 26.6$ Hz, $RhCH_2$), 9.195 (s, Cp*Me*), 14.906 (d, $J_{P-C} = 31.6$ Hz, $PMe_3$), 98.441 (m, $C_5Me_5$) and 129.565 (d, $J_{Rh-C} = 6.3$ Hz, CN). $^{31}P\{^1H\}$ ($C_6D_6$): $\delta$ 3.465 (d, $J_{Rh-P} = 146$ Hz). Mass spec: $m/z = 434$. Anal. Calcd (found) for $C_{15}H_{27}NPRh$: C, 41.49 (41.52); H, 6.04 (6.11); N, 3.23 (3.11).

**Preparation of $(C_5Me_5)Rh(PMe_3)(CH_3)(CN)$ (4).** A Schlenk flask was charged with **1** (100 mg, 0.972 mmol) and 3 mL of benzene, and irradiated at room temperature for 1.5 h. Volatiles were then removed *in vacuo*, leaving **3** as a red/brown residue which was then dissolved in acetonitrile and heated at 80 °C for 3 d. Volatiles were again removed *in vacuo*, leaving **4** as an orange solid. $^1$H NMR ($C_6D_6$): $\delta$ 0.493 (dd, $J_{Rh-H} = 6.0$ Hz, $J_{P-H} = 2.3$ Hz, 3 H, $RhCH_3$), 0.985 (d, $J_{P-H} = 10.3$ Hz, 9 H, $PMe_3$), 1.514 (d, $J_{Rh-H} = 2.5$ Hz, 15 H, $C_5Me_5$). $^{13}C\{^1H\}$ ($CDCl_3$): $\delta$ −7.78 (dd, $J_{Rh-C} = 23.6$ Hz, $J_{P-C} = 12.45$ Hz, $RhCH_3$), 9.64 (s, $C_5Me_5$), 16.27 (d, 32.5 Hz, $PMe_3$), 99.02 (d, 3.0 Hz, $C_5Me_5$), 136.89 (dd, $J_{Rh-C} = 56.8$ Hz, $J_{P-C} = 26.3$ Hz, RhCN). $^{31}P\{^1H\}$ ($C_6D_6$): $\delta$ 8.70 (d, $J_{Rh-P} = 141.7$ Hz, $RhPMe_3$). Anal. Calcd (found) for $C_{15}H_{27}NPRh$: C, 50.71 (50.56); H, 7.66 (7.66); N, 3.94 (3.81).

**Preparation of $(C_5Me_5)Rh(PMe_3)(Ph)(CN)$ (5).** A solution of **1** (100 mg, 0.972 mmol) was dissolved in 3 mL of benzonitrile and irradiated for 60 min at RT. A $^1$H NMR spectrum was collected in neat benzonitrile showing three hydrides, indicating C−H activation at the ortho, meta, and para positions with rotamers. $^1$H NMR (neat benzonitrile): $\delta$ −12.86, −13.84, and −13.85. $^{31}P\{^1H\}$ NMR (neat benzonitrile): $\delta$ 9.29 (d, $J_{Rh-P} = 136.8$ Hz), 8.01 (d, $J_{Rh-P} = 146.9$ Hz), 7.60 (d, $J_{Rh-P} = 149.3$ Hz, **1**), 7.32 (d, $J_{Rh-P} = 148.7$ Hz), 3.76 (d, $J_{Rh-P} = 149.3$ Hz), 1.74 (d, $J_{Rh-P} = 146.9$ Hz). This mixture was then heated at 100 °C for 24 h. Benzonitrile was then removed by prep TLC using a 1:1 THF/hexane as eluent. Compound **5** was then isolated and fully characterized. $^1$H NMR ($CDCl_3$): $\delta$ 1.35 (d, $J_{Rh-H} = 10.6$ Hz, $PMe_3$), 1.74 (d, $J_{Rh-H} = 2.7$ Hz, $C_5Me_5$), 6.93 (m, meta and para phenyl-H), 7.42 (b, ortho phenyl-H). $^{31}P\{^1H\}$ NMR ($CDCl_3$): $\delta$ 13.02 (d, $J_{Rh-P} = 140.8$ Hz). $^{13}C\{^1H\}$ ($CDCl_3$): $\delta$ 9.81 (s, $C_5Me_5$), 16.19 (d, $J_{C-P} = 33.8$ Hz, $PMe_3$), 100.40 (s, $C_5Me_5$), 122.79 (s, para), 128.17 (s, meta), 138.39 (dd, $J = 30.2$, 58.6 Hz, ipso-carbon), 140.70 (b, ortho), 153.36 (dd, $J = 17.7$, 31.2, Rh-CN). Anal. Calcd (found) for $C_{20}H_{29}NPRh \cdot 1/2THF$: C, 58.28 (58.31); H, 7.34 (7.94); N, 3.09 (3.00).

**Determining Reversibility for Isomerization of Compound 2 to 4.** A solution of **1** (15 mg, 0.047 mmol) in 0.4 mL of benzene was placed in an NMR tube sealed with a Teflon cap. This sample was irradiated for 1.5 h at room temperature. The solvent was immediately removed *in vacuo*, and the resulting red/brown residue dissolved in acetonitrile. This new reaction mixture was heated in an oil bath at 60 °C for 3 h. The solvent was then removed *in vacuo*, leaving a red/brown residue which was redissolved in acetonitrile-$d_3$ and returned to the 60 °C oil bath. The reaction progress was monitored by $^1$H and $^{31}P\{^1H\}$ NMR spectroscopy. The area of the Rh−*Me* ($\delta$ = 0.493) resonance was monitored over time in the $^1$H NMR spectrum. In the $^{31}P\{^1H\}$ NMR spectrum the disappearance of the **2** was observed along with the appearance of **4**.

**X-ray Crystal Structure Determinations.** Data were collected for compounds **2-Br**, **4**, and **5** on a Bruker SMART APEX II CCD Platform diffractometer at 100.0(1) K. The data collection was carried out using Mo Kα radiation. The intensity data were corrected for absorption. The structures were solved using SIR 97[26] and refined using SHELXL-97.[27] All non-hydrogen atoms were refined with anisotropic displacement parameters. All hydrogen atoms were found from the difference Fourier map and refined independently from the carbon atoms with individual isotropic displacement parameters. See Supporting Information for details.

**Acknowledgment.** We acknowledge the U.S. Department of Energy Office of Basic Sciences for their support of this work (Grant 86-ER-13569), and Dr. William Brennessel at the X-ray Crystallographic Facility of the Department of Chemistry at the University of Rochester. The Center for Enabling New Technologies through Catalysis (CENTC) Elemental Analysis Facility is also acknowledged for the use of its analytical facility (CHE-0650456).

**Supporting Information Available:** Tables of NMR data, X-ray crystallographic data for complexes **2-Br**, **4**, and **5** (CCDC nos. 789852−789854), coordinates and energies for calculated complexes, complete reference 21, and movies of transition states. This material is available free of charge via the Internet at http://pubs.acs.org.

JA107927B

(25) Barone, V.; Cossi, M.; Tomasi, J. *J. Chem. Phys.* **1997**, *107*, 3210.

(26) Altomare, A.; Burla, M. C.; Camalli, M.; Cascarano, G. L.; Giacovazzo, C.; Guagliardi, A.; Moliterni, A. G. G.; Polidori, G.; Spagna, R. *SIR97: A new program for solving and refining crystal structures*; Istituto di Cristallografia, CNR: Bari, Italy, 1999.

(27) Sheldrick, G. M. *Acta Crystallogr.* **2008**, *A64*, 112.